HHS Public Access

Author manuscript

Mol Pharm. Author manuscript; available in PMC 2023 July 04.

Published in final edited form as:

Mol Pharm. 2022 July 04; 19(7): 2535–2541. doi:10.1021/acs.molpharmaceut.2c00211.

Novel ^{64}Cu-Labeled NOTA-Conjugated Lactam-Cyclized Alpha-Melanocyte-Stimulating Hormone Peptides with Enhanced Tumor to Kidney Uptake Ratios

Zheng Qiao[1], **Jingli Xu**[1], **Rene Gonzalez**[2], **Yubin Miao**[1]

[1]Department of Radiology, University of Colorado Denver, Aurora, CO 80045, USA

[2]Department of Medical Oncology, University of Colorado Denver, Aurora, CO 80045, USA

Abstract

The aim of this study was to evaluate the effect of linker on tumor targeting and biodistribution of ^{64}Cu-NOTA-PEG$_2$Nle-CycMSH$_{hex}$ {^{64}Cu-1,4,7-triazacyclononane-1,4,7-triyl-triacetic acid-polyethylene glycol-Nle-c[Asp-His-DPhe-Arg-Trp-Lys]-CONH$_2$} and ^{64}Cu-NOTA-AocNle-CycMSH$_{hex}$ {^{64}Cu-NOTA-8-aminooctanoic acid-Nle-CycMSH$_{hex}$} on melanoma-bearing mice. NOTA-PEG$_2$Nle-CycMSH$_{hex}$ and NOTA-AocNle-CycMSH$_{hex}$ were synthesized and purified by HPLC. The melanocortin-1 (MC1) receptor binding affinities of the peptides were examined on B16/F10 melanoma cells. The biodistribution of ^{64}Cu-NOTA-PEG$_2$Nle-CycMSH$_{hex}$ and ^{64}Cu-NOTA-AocNle-CycMSH$_{hex}$ were determined on B16/F10 melanoma-bearing C57 mice. The melanoma imaging property of ^{64}Cu-NOTA-PEG$_2$Nle-CycMSH$_{hex}$ was further examined on B16/F10 melanoma-bearing C57 mice because of its higher melanoma uptake than ^{64}Cu-NOTA-AocNle-CycMSH$_{hex}$. The IC$_{50}$ values of NOTA- PEG$_2$Nle-CycMSH$_{hex}$ and NOTA-AocNle-CycMSH$_{hex}$ were 1.24 ± 0.07 and 2.75 ± 0.48 nM on B10/F10 melanoma cells. ^{64}Cu-NOTA-PEG$_2$Nle-CycMSH$_{hex}$ and ^{64}Cu-NOTA-AocNle-CycMSH$_{hex}$ were readily prepared with more than 90% radiolabeling yields and showed MC1R-specific binding on B16/F10 cells. ^{64}Cu-NOTA-PEG$_2$Nle-CycMSH$_{hex}$ exhibited higher tumor uptake than ^{64}Cu-NOTA-AocNle-CycMSH$_{hex}$ at 0.5, 2, 4 and 24 h post-injection. The tumor uptake of ^{64}Cu-NOTA-PEG$_2$Nle-CycMSH$_{hex}$ was 16.23 ± 0.42, 19.59 ± 1.48, 12.83 ± 1.69 and 8.78 ± 2.29% ID/g at 0.5, 2, 4 and 24 h post-injection, respectively. Normal organ uptake of ^{64}Cu-NOTA-PEG$_2$Nle-CycMSH$_{hex}$ was lower than 2% ID/g at 2 h post-injection except for kidney uptake. The renal uptake of ^{64}Cu-NOTA-PEG$_2$Nle-CycMSH$_{hex}$ was 3.66 ± 0.52, 3.27 ± 0.52 and 1.47 ± 0.56 ID/g at 2, 4 and 24 h post-injection, respectively. ^{64}Cu-NOTA-PEG$_2$Nle-CycMSH$_{hex}$ showed high tumor to normal organ uptake ratios after 2 h post-injection. The B16/F10 melanoma lesions could be clearly visualized by positron emission tomography (PET) using ^{64}Cu-NOTA-PEG$_2$Nle-CycMSH$_{hex}$ as an imaging probe at 2 h post-injection. High tumor uptake and low kidney uptake of ^{64}Cu-NOTA-PEG$_2$Nle-CycMSH$_{hex}$ underscored its potential as an MC1R-targeted theranostic peptide for melanoma imaging and therapy.

Graphical Abstract

Corresponding Author: Yubin Miao, 12700 East 19th Ave., MS C278, Department of Radiology, School of Medicine, University of Colorado Denver, Aurora, CO 80045, USA. Phone: (303) 724-3763; yubin.miao@cuanschutz.edu.

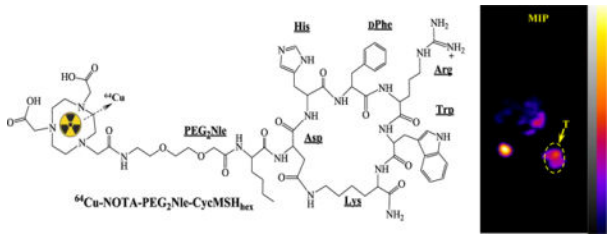

Keywords

^{64}Cu-NOTA; lactam-cyclized; alpha-melanocyte-stimulating hormone; melanocortin-1 receptor; melanoma imaging and therapy

INTRODUCTION

As the most lethal form of skin cancer, the financial burden of treating malignant melanoma continues to increase. Approximately 106,110 newly diagnosed cases and 7,180 deaths occurred in the United States in 2021. The 5-year survival of metastatic melanoma patients is only 35% although the new treatments (Vemurafenib, Ipilimumab and Nivolumab) have increased the overall survival of by months (2–7). Melanocortin-1 receptor (MC1R) is a G protein-coupled receptor which over-expresses on both amelanotic and melanotic human melanomas (8–10). Alpha-melanocyte-stimulating hormone (α-MSH) peptides can bind to MC1Rs with nanomolar binding affinities (11–23). Thus, numerous research efforts have been dedicated to the development of theranostic MC1R-targeted α-MSH peptides for melanoma imaging and therapy (11–23).

Building upon the lactam-cyclized key sequence of Gly-Gly-Nle-c[Asp-His-DPhe-Arg-Trp-Lys]-$CONH_2$ (GGNle-$CycMSH_{hex}$), we have conjugated both diagnostic and therapeutic radionuclides to yield a novel class of MC1R-targeted radiolabeled α-MSH peptides. For instance, our ^{68}Ga-DOTA-GGNle-$CycMSh_{hex}$ displayed a B16/F10 melanoma uptake of 24.27 ± 3.74% ID/g at 1 h post-injection (10). Furthermore, ^{68}Ga-DOTA-GGNle-$CycMSH_{hex}$ clearly detected human metastatic melanoma lesions in brain, lung, connective tissue and intestines (10). The remarkable images of melanoma metastases in patients by ^{68}Ga-DOTA-GGNle-$CycMSH_{hex}$ highlighted the clinical relevance of MC1R for melanoma imaging and therapy.

Copper-64 ($t_{1/2}$=12.7 h, 17.4% β^+, 40% β^-) is an attractive theranostic radionuclide because of the emissions of positrons and beta-particles. In our previous work, ^{64}Cu-NOTA-GGNle-$CycMSH_{hex}$ {^{64}Cu-1,4,7-triazacyclononane-1,4,7-triacetic acid- GGNle-$CycMSH_{hex}$) displayed B16/F1 melanoma uptake of 12.39 ± 1.61% ID/g and 12.71 ± 2.68% ID/g at 2 h and 4 h post-injection (14). The melanoma lesions could be clearly imaged by positron emission tomography (PET) using ^{64}Cu-NOTA-GGNle-$CycMSH_{hex}$ as an imaging probe (14). Furthermore, we reported that the replacement of the -GG- linker with 8-aminooctanoic acid (Aoc) linker increased the uptake of ^{99m}Tc(EDDA)-hydrazinonicotinamide (HYNIC)-AocNle-$CycMSH_{hex}$ in melanoma by more than 60% at 2 h and 4 h post-injection (15, 16). Therefore, we were interested whether the replacement

of the -GG- linker with Aoc or polyethylene glycol (PEG) linker could affect the melanoma uptake of the ^{64}Cu-labeled NOTA-conjugated CycMSH$_{hex}$ peptides.

In this study, we synthesized NOTA-AocNle-CycMSH$_{hex}$ and NOTA-PEG$_2$Nle-CycMSH$_{hex}$ using standard Fluorenylmethyloxycarbonyl (Fmoc) chemistry, radiolabeled both peptides with ^{64}Cu, and determined their melanoma targeting and biodistribution properties on B16/F10 melanoma-bearing C57 mice. Because ^{64}Cu-NOTA-PEG$_2$Nle-CycMSH$_{hex}$ displayed higher tumor uptake than ^{64}Cu-NOTA-AocNle-CycMSH$_{hex}$ at all time points investigated, we further examined the melanoma imaging of ^{64}Cu-NOTA-PEG$_2$Nle-CycMSH$_{hex}$ on B16/F10 melanoma-bearing C57 mice.

Experimental Section

Chemicals and Reagents

Amino acids and resin were purchased from Advanced ChemTech Inc. (Louisville, KY) and Novabiochem (San Diego, CA). NOTA(OtBu)$_2$ was purchased from CheMatech Inc. (Dijon, France) for peptide synthesis. ^{125}I-Tyr^2-[Nle^4, D-Phe^7]-α-MSH {^{125}I-(Tyr^2)-NDP-MSH} was obtained from PerkinElmer, Inc. (Waltham, MA) for competitive receptor binding assay. ^{64}CuCl$_2$ was purchased from Washington University School of Medicine (St. Louis, MO) for radiolabeling. B16/F10 murine melanoma cells were received from American Type Culture Collection (Manassas, VA). All other chemicals used in this study were purchased from Thermo Fisher Scientific (Waltham, MA) and used as received without further purification.

Peptide Synthesis and Receptor Binding Assay

NOTA-PEG$_2$Nle-CycMSH$_{hex}$ and NOTA-AocNle-CycMSH$_{hex}$ were synthesized on Sieber amide resin using standard Fmoc chemistry according to the procedure described in our previous publication (14). The peptides were purified by reverse phase-high performance liquid chromatography (RP-HPLC) and characterized by liquid chromatography-mass spectrometry (LC-MS). The MC1 receptor binding affinities of NOTA-PEG$_2$Nle-CycMSH$_{hex}$ and NOTA-AocNle-CycMSH$_{hex}$ were determined on B16/F10 melanoma cells by *in vitro* competitive receptor binding assay in the presence of 10^{-13} to 10^{-5} M of each peptide according to our published procedure (14). The IC$_{50}$ values were calculated using the Prism software (GraphPad Software, La Jolla, CA, USA).

Radiolabeling

^{64}Cu-NOTA-PEG$_2$Nle-CycMSH$_{hex}$ and ^{64}Cu-NOTA-AocNle-CycMSH$_{hex}$ were prepared as described in our previous publication (14). The proposed schematic structures of ^{64}Cu-NOTA-PEG$_2$Nle-CycMSH$_{hex}$ and ^{64}Cu-NOTA-AocNle-CycMSH$_{hex}$ are shown in Figure 1. Briefly, 10 μL of ^{64}CuCl$_2$ (37–74 MBq in 0.05 M HCl aqueous solution), 10 μL of 1 mg/mL peptide aqueous solution, and 200 μL of 0.5 M NH$_4$OAc (pH 5.4) were added into a reaction vial and incubated at 75 °C for 1 h. After incubation, 10 μL of 0.5% EDTA aqueous solution was added to scavenge potentially unbound ^{64}Cu^{2+}. ^{64}Cu-NOTA-PEG$_2$Nle-CycMSH$_{hex}$ and ^{64}Cu-NOTA-AocNle-CycMSH$_{hex}$ complexes were purified by Waters RP-HPLC (Milford, MA) on a Grace Vydac C-18 reverse phase analytical column (Deerfield, IL) with a flow

rate of 1 mL/min. A 20 min gradient of 20–30% acetonitrile in 20 mM HCl aqueous solution was used for ^{64}Cu-NOTA-PEG$_2$Nle-CycMSH$_{hex}$, whereas a 20 min gradient of 24–34% acetonitrile in 20 mM HCl aqueous solution was utilized for ^{64}Cu-NOTA-AocNle-CycMSH$_{hex}$. Each purified peptide solution was purged with N_2 gas for 15 min to remove the acetonitrile, then adjusted to pH 7.4 with 0.1 M NaOH and sterile saline for animal studies.

Specific Binding

Specific binding of ^{64}Cu-NOTA-PEG$_2$Nle-CycMSH$_{hex}$ and ^{64}Cu-NOTA-AocNle-CycMSH$_{hex}$ was determined on B16/F10 cells seeded on 24-well plates. The B16/F10 melanoma cells (1×10^6 cells per well, n = 3) were incubated at 25 °C for 1 h with approximately 22.2 KBq of ^{64}Cu-NOTA-PEG$_2$Nle-CycMSH$_{hex}$ or ^{64}Cu-NOTA-AocNle-CycMSH$_{hex}$ with or without 10 μg (6.07 nmol) of unlabeled [Nle^4, D-Phe^7]-α-MSH (NDP-MSH) in 0.3 mL of binding medium {Dulbecco's modified Eagle's medium with 25 mM *N*-(2-hydroxyethyl)-piperazine-*N'*-(2-ethanesulfonic acid), pH 7.4, 0.2% bovine serum albumin (BSA), 0.3 mM 1,10-phenathroline}. The binding medium was aspirated after incubation. The cells were washed twice with 0.5 mL of ice-cold 0.01 M phosphate buffered saline (PBS) buffer containing 0.2% BSA (pH = 7.4), and lysed with 0.5 mL of 1 M NaOH for 5 min, collected and measured in a Wallac 1480 automated gamma counter (PerkinElmer, NJ).

Biodistribution and Imaging Studies

All animal studies were conducted in compliance with Institutional Animal Care and Use Committee approval. C57 mice were purchased from Charles River Laboratory (Wilmington, MA). Each C57 mouse was subcutaneously inoculated with 1×10^6 B16/F10 cells on the right flank to generate melanoma tumors. Ten days post inoculation, the tumor weights reached about 0.2 g and the melanoma-bearing C57 mice were used for biodistribution and PET imaging studies. Each melanoma-bearing mouse was injected with 0.37 MBq of ^{64}Cu-NOTA-PEG$_2$Nle-CycMSH$_{hex}$ or ^{64}Cu-NOTA-AocNle-CycMSH$_{hex}$ *via* the tail vein. The specificity of the tumor uptake of ^{64}Cu-NOTA-PEG$_2$Nle-CycMSH$_{hex}$ and ^{64}Cu-NOTA-AocNle-CycMSH$_{hex}$ was determined by co-injecting 10 μg (6.07 nmol) of unlabeled NDP-MSH. Mice were sacrificed at 0.5, 2, 4 and 24 h post-injection, and tumors and organs of interest were harvested, weighted and counted. Blood value was taken as 6.5% of the whole-body weight.

Since ^{64}Cu-NOTA-PEG$_2$Nle-CycMSH$_{hex}$ displayed higher tumor uptake than ^{64}Cu-NOTA-AocNle-CycMSH$_{hex}$, the melanoma imaging property of ^{64}Cu-NOTA-PEG$_2$Nle-CycMSH$_{hex}$ was examined on B16/F10 melanoma-bearing C57 mice. Each mouse was injected with 7.4 MBq of ^{64}Cu-NOTA-PEG$_2$Nle-CycMSH$_{hex}$ *via* the tail vein. PET imaging studies of melanoma-bearing mice were performed at 2 h post-injection. Reconstructed PET data was visualized using VivoQuant (Invicro, Boston, MA).

Statistical Analysis

Statistical analysis was performed using the Student's *t* test for unpaired data. A 95% confidence level was chosen to determine the significance of difference in tumor and kidney

uptake between ^{64}Cu-NOTA-PEG$_2$Nle-CycMSH$_{hex}$ with/without NDP-MSH blockade, tumor and kidney uptake between ^{64}Cu-NOTA-AocNle-CycMSH$_{hex}$ with/without NDP-MSH blockade. The differences at the 95% confidence level ($p < 0.05$) were considered significant.

Results

The schematic structures of NOTA-PEG$_2$Nle-CycMSH$_{hex}$ and NOTA-AocNle-CycMSH$_{hex}$ are presented in Figure 1. Both peptides were synthesized, purified by HPLC and displayed greater than 90% purities after HPLC purification. The identities of the peptides were confirmed by mass spectrometry. As shown in Table 1, the measured molecular weights of NOTA-PEG$_2$Nle-CycMSH$_{hex}$ and NOTA-AocNle-CycMSH$_{hex}$ matched their calculated molecular weights. The molecular weights of NOTA-PEG$_2$Nle-CycMSH$_{hex}$ and NOTA-AocNle-CycMSH$_{hex}$ were 1412 and 1408. The IC$_{50}$ values of NOTA-PEG$_2$Nle-CycMSH$_{hex}$ and NOTA-AocNle-CycMSH$_{hex}$ were 1.24 ± 0.07 and 2.75 ± 0.48 nM on B10/F10 cells.

^{64}Cu-NOTA-PEG$_2$Nle-CycMSH$_{hex}$ and ^{64}Cu-NOTA-AocNle-CycMSH$_{hex}$ were prepared in 0.5 M NH_4OAc-buffered solution with the greater than 90% radiochemical yields. Radioactive HPLC profiles of ^{64}Cu-NOTA-PEG$_2$Nle-CycMSH$_{hex}$ and ^{64}Cu-NOTA-AocNle-CycMSH$_{hex}$ are shown in Figure 2. The retention time of ^{64}Cu-NOTA-PEG$_2$Nle-CycMSH$_{hex}$ and ^{64}Cu-NOTA-AocNle-CycMSH$_{hex}$ was 12.3 and 12.7 min, respectively. The specific activity was 2.36×10^4 mCi/μmol for ^{64}Cu-NOTA-PEG$_2$Nle-CycMSH$_{hex}$ and ^{64}Cu-NOTA-AocNle-CycMSH$_{hex}$. As shown in Figure 2B, both ^{64}Cu-NOTA-PEG$_2$Nle-CycMSH$_{hex}$ and ^{64}Cu-NOTA-AocNle-CycMSH$_{hex}$ exhibited MC1R-specific binding. The peptide blockade reduced 92% of ^{64}Cu-NOTA-PEG$_2$Nle-CycMSH$_{hex}$ and 70% of ^{64}Cu-NOTA-AocNle-CycMSH$_{hex}$ cellular uptake.

Table 2 and Table 3 showed the biodistribution results of ^{64}Cu-NOTA-PEG$_2$Nle-CycMSH$_{hex}$ and ^{64}Cu-NOTA-AocNle-CycMSH$_{hex}$. ^{64}Cu-NOTA-PEG$_2$Nle-CycMSH$_{hex}$ displayed rapid melanoma uptake and prolonged tumor retention. The tumor uptake of ^{64}Cu-NOTA-PEG$_2$Nle-CycMSH$_{hex}$ was 16.23 ± 0.42, 19.59 ± 1.48, 12.83 ± 1.69 and 8.78 ± 2.29% ID/g at 0.5, 2, 4 and 24 h post-injection, respectively. Approximately 88% of tumor uptake of ^{64}Cu-NOTA-PEG$_2$Nle-CycMSH$_{hex}$ was blocked by 10 μg (6.07 nmol) of NDP-MSH ($P<0.05$), suggesting that the tumor uptake was MC1R-mediated. Normal organ uptake of ^{64}Cu-NOTA-PEG$_2$Nle-CycMSH$_{hex}$ was lower than 2% ID/g at 2 h post-injection except for kidney uptake (3.66 ± 0.52% ID/g).

^{64}Cu-NOTA-AocNle-CycMSH$_{hex}$ exhibited lower tumor uptake than ^{64}Cu-NOTA-PEG$_2$Nle-CycMSH$_{hex}$ at all time points investigated. The tumor uptake of ^{64}Cu-NOTA-AocNle-CycMSH$_{hex}$ was 5.69 ± 0.23, 7.71 ± 0.67, 5.47 ± 0.52 and 1.54 ± 0.16% ID/g at 0.5, 2, 4 and 24 h post-injection, respectively. Approximately 74% of tumor uptake of ^{64}Cu-NOTA-AocNle-CycMSH$_{hex}$ was decreased by 10 μg (6.07 nmol) of NDP-MSH blockade ($P<0.05$), indicating that the tumor uptake was MC1R-specific. Normal organ uptake of ^{64}Cu-NOTA-PEG$_2$Nle-CycMSH$_{hex}$ was lower than 2.2% ID/g at 2 h post-injection except for kidney uptake (3.29 ± 0.61% ID/g).

^{64}Cu-NOTA-PEG$_2$Nle-CycMSH$_{hex}$ showed higher tumor/kidney and tumor/liver ratios than ^{64}Cu-NOTA-AocNle-CycMSH$_{hex}$. Thus, we further performed PET imaging of ^{64}Cu-NOTA-PEG$_2$Nle-CycMSH$_{hex}$ on B16/F10 melanoma-bearing mice. The representative maximum intensity projection (MIP) and coronal PET images of Al^{18}F-NOTA-PEG$_2$Nle-CycMSH$_{hex}$ on B16/F10 melanoma-bearing C57 mice are presented in Figure 3. In agreement with biodistribution result, the B16/F10 tumor lesions were clearly imaged at 2 h post-injection using ^{64}Cu-NOTA-PEG$_2$Nle-CycMSH$_{hex}$ as imaging probe.

Discussion

We demonstrated that the substitution of DOTA with NOTA dramatically improved the uptake in melanoma and decreased the kidney uptake of ^{64}Cu-NOTA-GGNle-CycMSH$_{hex}$ as compared to ^{64}Cu-DOTA-GGNle-CycMSH$_{hex}$ (14). The higher melanoma uptake and lower renal uptake of ^{64}Cu-NOTA-GGNle-CycMSH$_{hex}$ improved the tumor to kidney uptake ratios of ^{64}Cu-NOTA-GGNle-CycMSH$_{hex}$ (14). Thus, NOTA is a better suited for ^{64}Cu chelation. Interestingly, we also reported that the switch from the -GG- linker to Aoc linker improved the melanoma uptake of ^{99m}Tc(EDDA)-HYNIC-AocNle-CycMSH$_{hex}$ by greater than 60% at 2 h and 4 h post-injection as compared to ^{99m}Tc(EDDA)-HYNIC-GGNle-CycMSH$_{hex}$ (15, 16). Meanwhile, ^{99m}Tc(EDDA)-HYNIC-PEG$_2$Nle-CycMSH$_{hex}$ exhibited similar melanoma and renal uptake as ^{99m}Tc(EDDA)-HYNIC-AocNle-CycMSH$_{hex}$ (15, 16). Therefore, we were interested in the effect of PEG$_2$ and Aoc linkers on tumor targeting and biodistribution of ^{64}Cu-NOTA-PEG$_2$Nle-CycMSH$_{hex}$ and ^{64}Cu-NOTA-AocNle-CycMSH$_{hex}$ on melanoma-bearing mice in this study.

NOTA-PEG$_2$Nle-CycMSH$_{hex}$ exhibited slightly stronger MC1R binding affinity than NOTA-AocNle-CycMSH$_{hex}$ on B16/F10 cells (1.24 vs. 2.75 nM). Similarly, ^{64}Cu-NOTA-PEG$_2$Nle-CycMSH$_{hex}$ displayed greater MC1R-speific cellular uptake than ^{64}Cu-NOTA-AocNle-CycMSH$_{hex}$ on B16/F10 cells. The cellular uptake of ^{64}Cu-NOTA-PEG$_2$Nle-CycMSH$_{hex}$ was 2.8 times the uptake of ^{64}Cu-NOTA-AocNle-CycMSH$_{hex}$ (Fig. 2). Furthermore, ^{64}Cu-NOTA-PEG$_2$Nle-CycMSH$_{hex}$ exhibited more tumor uptake than ^{64}Cu-NOTA-AocNle-CycMSH$_{hex}$ on B16/F10 melanoma-bearing mice. The tumor uptake of ^{64}Cu-NOTA-PEG$_2$Nle-CycMSH$_{hex}$ was 2.9, 2.5, 2.3 and 5.7 times the uptake of ^{64}Cu-NOTA-AocNle-CycMSH$_{hex}$ at 0.5, 2, 4 and 24 h post-injection (Tables 2 and 3). The uptake in kidneys and liver was comparably low for both ^{64}Cu-NOTA-PEG$_2$Nle-CycMSH$_{hex}$ and ^{64}Cu-NOTA-AocNle-CycMSH$_{hex}$ after 2 h post-injection. Interestingly, ^{99m}Tc(EDDA)-HYNIC-AocNle-CycMSH$_{hex}$ showed 60% higher melanoma uptake than ^{99m}Tc(EDDA)-HYNIC-PEG$_2$Nle-CycMSH$_{hex}$ at 2 h post-injection in our previous publications (15, 16), suggesting that the moiety of radiometal-chelator and the linker attached to the receptor-targeted peptide could affect the tumor uptake of radiolabeled peptides.

At the present time, ^{64}Cu-NOTA-GGNle-CycMSH$_{hex}$ displayed the highest tumor/kidney ratios among all reported MC1R-targeted ^{64}Cu-labeled α-MSH peptides (14, 21–23). As shown in Fig. 4, ^{64}Cu-NOTA-PEG$_2$Nle-CycMSH$_{hex}$ displayed higher tumor/kidney ratios than ^{64}Cu-NOTA-GGNle-CycMSH$_{hex}$ at 2, 4 and 24 h post-injection. The tumor uptake of ^{64}Cu-NOTA-PEG$_2$Nle-CycMSH$_{hex}$ was 1.6 and 2.1 times the tumor uptake of ^{64}Cu-NOTA-GGNle-CycMSH$_{hex}$ at 2 h and 4 h post-injection. The B16/F10 melanoma lesions could be

clearly visualized using ^{64}Cu-NOTA-PEG$_2$Nle-CycMSH$_{hex}$ as an imaging probe (Fig. 3). It is worthwhile to note that ^{64}Cu is also a therapeutic radionuclide with beta-emissions. The improved tumor/kidney uptake ratios of ^{64}Cu-NOTA-PEG$_2$Nle-CycMSH$_{hex}$ would potentially facilitate its application in melanoma therapy.

Over the past several years, various VLA-4-targeted (integrin $\alpha_4\beta_1$-targeted) ^{64}Cu-labeled LLP2A peptides were developed and evaluated for melanoma targeting (24, 25). For instance, CB-TE1A1P (1,4,8,11-tetraazacyclotetradecane-1-(methane phosphonic acid)-8-(methane carboxylic acid), 2-(4,7-bis(carboxymethyl)-1,4,7-triazonan-1-yl)pentanedioic acid (NODAGA) and 4,11-bis(carboxymethyl)-1,4,8,11-tetraazabicyclo[6.6.2]hexadecane (CB-TE2A) were conjugated to the LLP2A peptide for ^{64}Cu chelation (24, 25). Among these reported ^{64}Cu-labeled LLP2A peptides, ^{64}Cu-CB-TE1A1P-PEG$_4$-LLP2A showed the highest B16/F10 melanoma uptake, with 15.1 ± 1.0% ID/g and 16.9 ± 2.2% ID/g at 2 h and 4 h post-injection (25). As demonstrated in this study, ^{64}Cu-NOTA-PEG$_2$Nle-CycMSH$_{hex}$ exhibited similar uptake in tumor, liver and kidneys as ^{64}Cu-CB-TE1A1P-PEG$_4$-LLP2A. Meanwhile, ^{64}Cu-CB-TE1A1P-PEG$_4$-LLP2A also displayed high VLA-4-specific uptake in normal lung, bone and spleen (4.6–18.1% ID/g at 2 h post-injection) (25), whereas the uptake of ^{64}Cu-NOTA-PEG$_2$Nle-CycMSH$_{hex}$ was extremely low in these normal organs (<0.7% ID/g at 2 h post-injection). Low accumulation of ^{64}Cu-NOTA-PEG$_2$Nle-CycMSH$_{hex}$ in normal lung and bone would potentially facilitate the imaging of melanoma metastases in these organs. From the therapeutic point of view, the enhanced tumor/kidney and tumor/liver uptake ratios of ^{64}Cu-NOTA-PEG$_2$Nle-CycMSH$_{hex}$ would potentially increase the absorbed dose to tumor while minimizing the absorbed dose to liver and kidneys when treating the melanoma with ^{64}Cu-NOTA-PEG$_2$Nle-CycMSH$_{hex}$ in future studies.

Conclusions

The melanoma targeting and biodistribution properties of ^{64}Cu-NOTA-PEG$_2$Nle-CycMSH$_{hex}$ and ^{64}Cu-NOTA-AocNle-CycMSH$_{hex}$ were determined on B16/F10 melanoma-bearing C57 mice. ^{64}Cu-NOTA-PEG$_2$Nle-CycMSH$_{hex}$ showed higher tumor uptake than ^{64}Cu-NOTA-AocNle-CycMSH$_{hex}$ at all time points investigated. The favorable biodistribution and imaging properties of ^{64}Cu-NOTA-PEG$_2$Nle-CycMSH$_{hex}$ underscored its potential as an MC1R-targeted theranostic peptide for melanoma imaging and therapy.

Acknowledgements

We thank Dr. Fabio Gallazzi and Jenna Steiner for their technical assistance. This work was supported by NIH Grant R01CA225837. PET imaging experiments were conducted in the University of Colorado Anschutz Medical Campus Animal Imaging Shared Resources supported in part by the University of Colorado Cancer Center (NCI P30 CA046934) and the Colorado Clinical and Translational Sciences Institute (NIH/NCATS UL1 TR001082).

References

1. Siegel RL; Miller KD; Fuchs HE, Jemal A Cancer statistics, 2021. CA Cancer J. Clin 2021, 71, 7–33. [PubMed: 33433946]
2. Chapman PB; Hauschild A; Robert C; et al. BRIM-3 Study Group. Improved survival with vemurafenib in melanoma with BRAF V600E mutation. N. Engl. J. Med 2011, 364, 2507–2516 . [PubMed: 21639808]

3. Sosman JA; Kim KB; Schuchter L; et al. Survival in BRAF V600-mutant advanced melanoma treated with vemurafenib. N. Engl. J. Med 2012, 366, 707–714. [PubMed: 22356324]
4. Hodi FS; O'Day SJ; McDermott DF; et al. Improved survival with ipilimumab in patients with metastatic melanoma. N. Engl. J. Med 2010, 363, 711–723. [PubMed: 20525992]
5. Weber JS; O'Day SJ; Urba W; et al. Phase I/II study of ipilimumab for patients with metastatic melanoma. J. Clin. Oncol 2008, 26, 5950–5956. [PubMed: 19018089]
6. Topalian SL; Sznol M; McDermott DF; et al. Survival, durable tumor remission, and long-term safety in patients with advanced melanoma receiving nivolumab. J. Clin. Oncol 2014, 32, 1020–1030. [PubMed: 24590637]
7. Weiss SA; Wolchok JD; Sznol M Immunotherapy of melanoma: facts and hopes. Clin. Cancer Res 2019, 25, 5191–5201. [PubMed: 30923036]
8. Siegrist W; Solca F; Stutz S; et al. Characterization of receptors for alpha-melanocyte-stimulating hormone on human melanoma cells. Cancer Res. 1989, 49, 6352–6358. [PubMed: 2804981]
9. Tatro JB; Wen Z; Entwistle ML; et al. Interaction on an α-melanocyte stimulating hormone-diptheria toxin fusion protein with melanotropin receptors in human metastases. Cancer Res. 1992, 52, 2545–2548. [PubMed: 1314697]
10. Yang J; Xu J; Gonzalez R; Lindner T; Kratochwil C; Miao Y ^{68}Ga-DOTA-GGNle-CycMSH$_{hex}$ targets the melanocortin-1 receptor for melamoma imaging. Sci. Transl. Med 2018, 10, eaau4445. [PubMed: 30404861]
11. Guo H; Yang J; Gallazzi F; Miao Y Reduction of the ring size of radiolabeled lactam bridge-cyclized alpha-MSH peptide resulting in enhanced melanoma uptake. J. Nucl. Med 2010, 51, 418–426. [PubMed: 20150256]
12. Guo H; Yang J; Gallazzi F; Miao Y Effects of the amino acid linkers on melanoma-targeting and pharmacokinetic properties of Indium-111-labeled lactam bridge-cyclized α-MSH peptides. J. Nucl. Med 2011, 52, 608–616. [PubMed: 21421725]
13. Guo H; Gallazzi F; Miao Y Ga-67-labeled lactam bridge-cyclized alpha-MSH peptides with enhanced melanoma uptake and reduced renal uptake. Bioconjug. Chem 2012, 23, 1341–1348. [PubMed: 22621181]
14. Guo H; Miao Y Cu-64-labeled lactam bridge-cyclized alpha-MSH peptides for PET imaging of melanoma. Mol. Pharm 2012, 9, 2322–2330. [PubMed: 22780870]
15. Guo H; Gallazzi F; Miao Y Design and evaluation of new Tc-99m-labeled lactam bridge-cyclized alpha-MSH peptides for melanoma imaging. Mol. Pharm 2013, 10, 1400–1408. [PubMed: 23418722]
16. Guo H; Miao Y Introduction of an aminooctanoic acid linker enhances uptake of Tc-99m-labeled lactam bridge-cyclized alpha-MSH peptide in melanoma. J. Nucl. Med 2014, 55, 2057–2063. [PubMed: 25453052]
17. Guo H; Miao Y Melanoma targeting property of a Lu-177-labeled lactam bridge-cyclized alpha-MSH peptide. Bioorg. Med. Chem. Lett 2013, 23, 2319–2323. [PubMed: 23473679]
18. Yang J; Xu J; Cheuy L; Gonzalez R; Fisher DR; Miao Y Evaluation of a novel Pb-203-labeled lactam-cyclized alpha-melanocyte-stimulating hormone peptide for melanoma targeting. Mol. Pharm 2019, 16, 1694–1702. [PubMed: 30763112]
19. Xu J; Yang J; Gonzalez R; Fisher DR; Miao Y Melanoma-targeting property of Y-90-labeled lactam-cyclized alpha-melanocyte-stimulating hormone peptide. Cancer Biother. Radiopharm 2019, 34, 597–603. [PubMed: 31644317]
20. Qiao Z, Xu J; Gonzalez R; Miao Y Novel [^{99m}Tc]-tricarbonyl-NOTA-conjugated lactam-cyclized alpha-MSH peptide with enhanced melanoma uptake and reduced renal uptake. Mol. Pharm 2020, 17, 3581–3588. [PubMed: 32663011]
21. McQuade P; Miao Y; Yoo J; Quinn TP; Welch MJ; Lewis JS Imaging of melanoma using 64Cu- and 86Y-DOTA-ReCCMSH(Arg11), a cyclized peptide analogue of alpha-MSH. J. Med. Chem 2005, 48, 2985–2992. [PubMed: 15828837]
22. Wei L; Butcher C; Miao Y; et al. Synthesis and biologic evaluation of ^{64}Cu-labeled rhenium-cyclized alpha-MSH peptide analog using a cross-bridged cyclam chelator. J. Nucl. Med 2007, 48, 64–72. [PubMed: 17204700]

23. Cheng Z; Xiong Z; Subbarayan M; Chen X; Gambhir SS ^{64}Cu-labeled alpha-melanocyte-stimulating hormone analog for MicroPET imaging of melanocortin 1 receptor expression. Bioconjugate Chem. 2007, 18, 765–772.

24. Jiang M; Ferdani R; Shokeen M; Anderson CJ Comparison of two cross-bridged macrocyclic chelators for the evaluation of 64Cu-labeled-LLP2A, a peptidomimetic ligand targeting VLA-4-positive tumors. Nucl. Med. Biol 2013, 40, 245–251. [PubMed: 23265977]

25. Beaino W; Anderson, C. J. PET imaging of very late antigen-4 in melanoma: comparison of ^{68}Ga- and ^{64}Cu-labeled NODAGA and CB-TE1A1P-LLP2A conjugates. J. Nucl. Med 2014, 55, 1856–1863. [PubMed: 25256059]

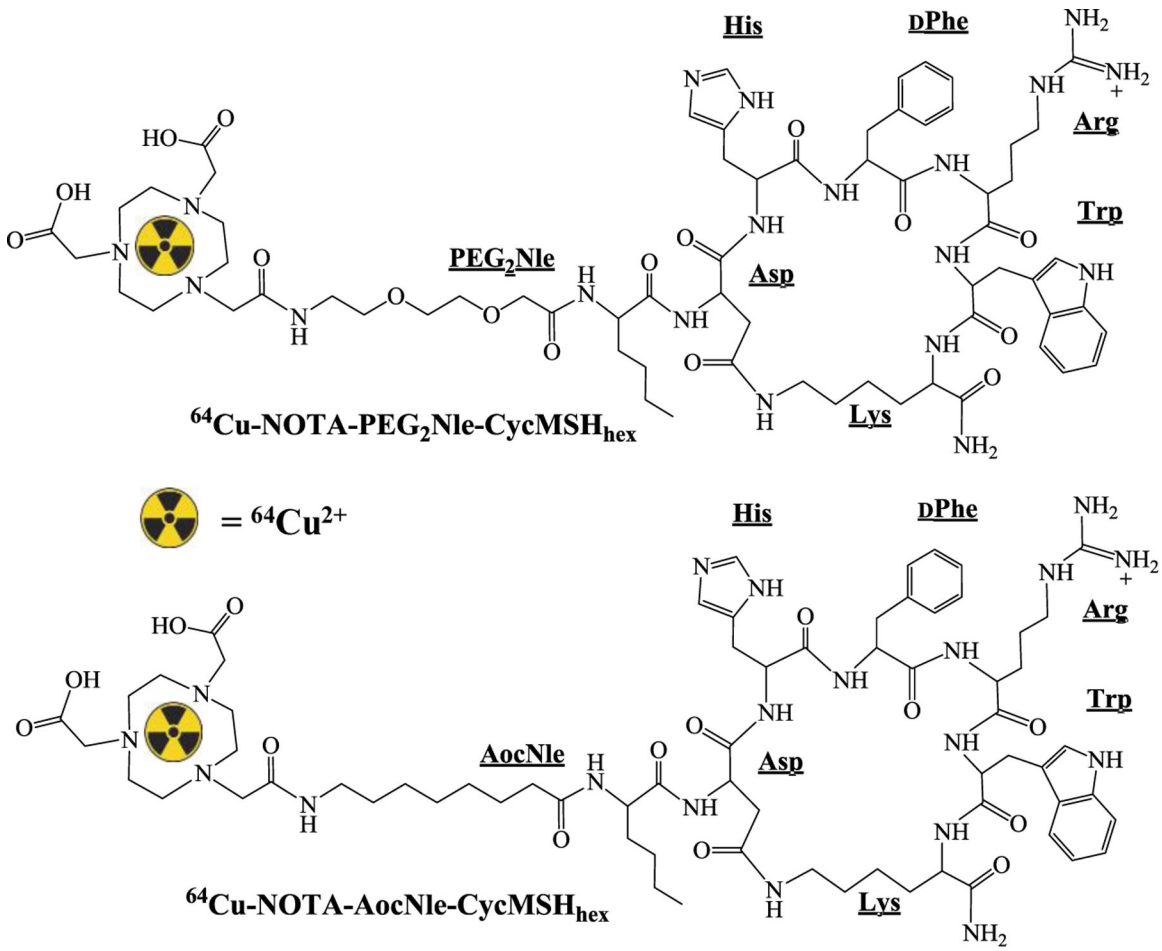

Figure 1.

Proposed schematic structures of ^{64}Cu-NOTA-PEG$_2$Nle-CycMSH$_{hex}$ and ^{64}Cu-NOTA-AocNle-CycMSH$_{hex}$.

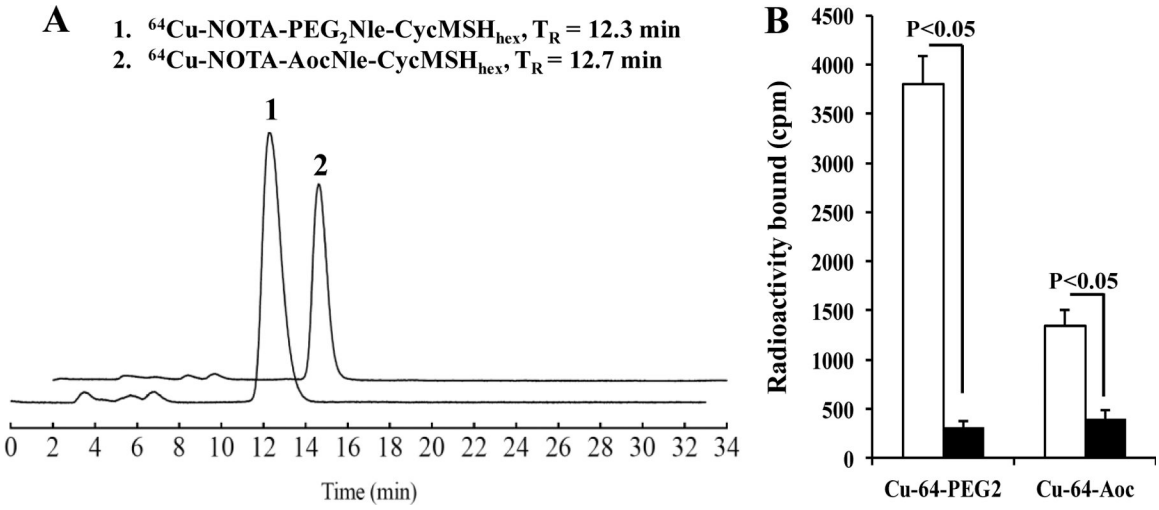

Figure 2.

A. Radioactive HPLC profiles of ^{64}Cu-NOTA-PEG$_2$Nle-CycMSH$_{hex}$ and ^{64}Cu-NOTA-AocNle-CycMSH$_{hex}$. B. Specific binding of ^{64}Cu-NOTA-PEG$_2$Nle-CycMSH$_{hex}$ (Cu-64-PEG$_2$) and ^{64}Cu-NOTA-AocNle-CycMSH$_{hex}$ (Cu-64-Aoc) on B16/F10 melanoma cells with (black) and without (white) peptide blockade, respectively.

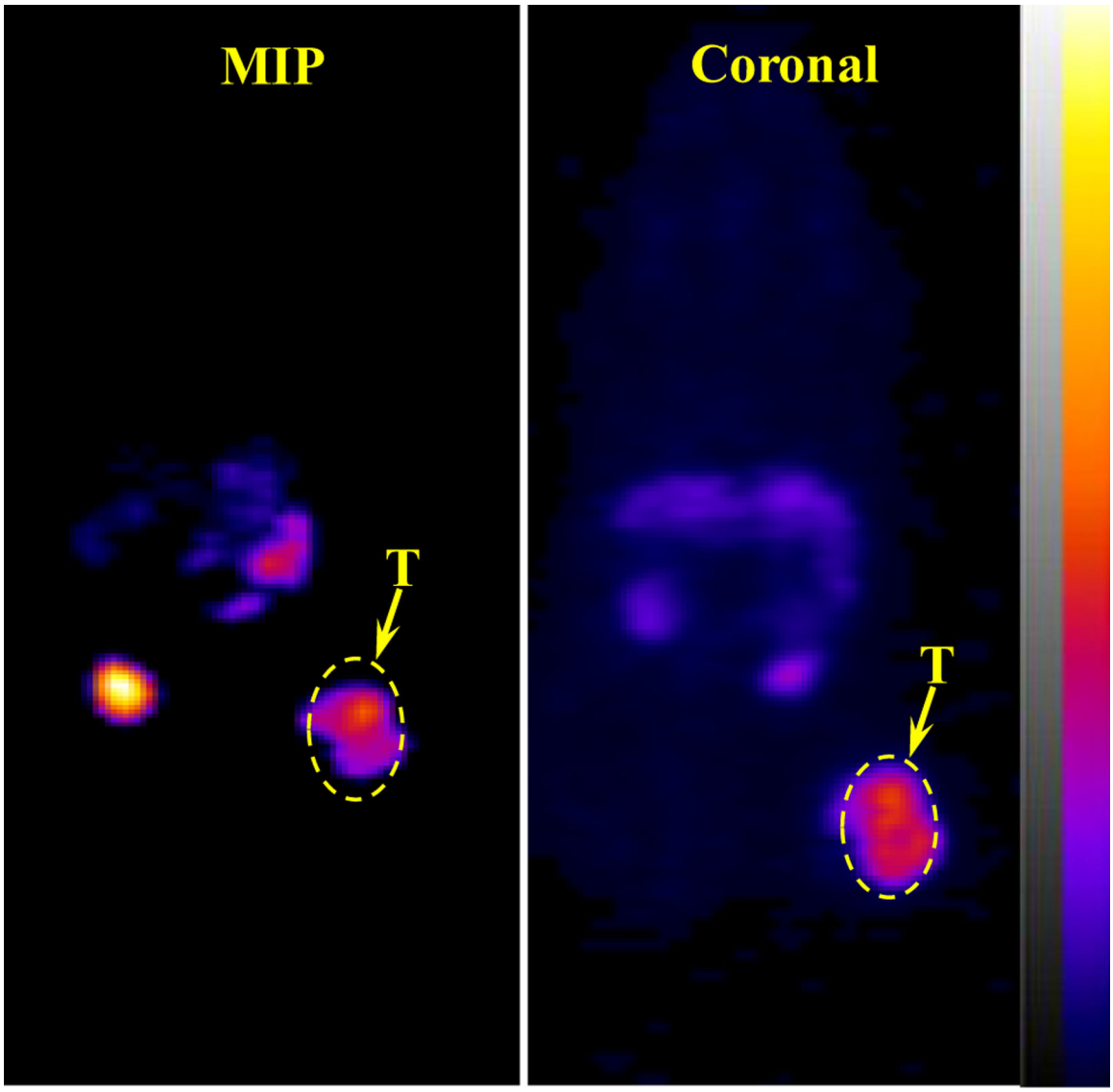

Figure 3.

Representative maximum intensity projection (MIP) and coronal PET images of ^{64}Cu-NOTA-PEG$_2$Nle-CycMSH$_{hex}$ on a B16/F10 melanoma-bearing C57 mouse at 2 h post-injection. The melanoma lesions (T) are highlighted with arrows on the images.

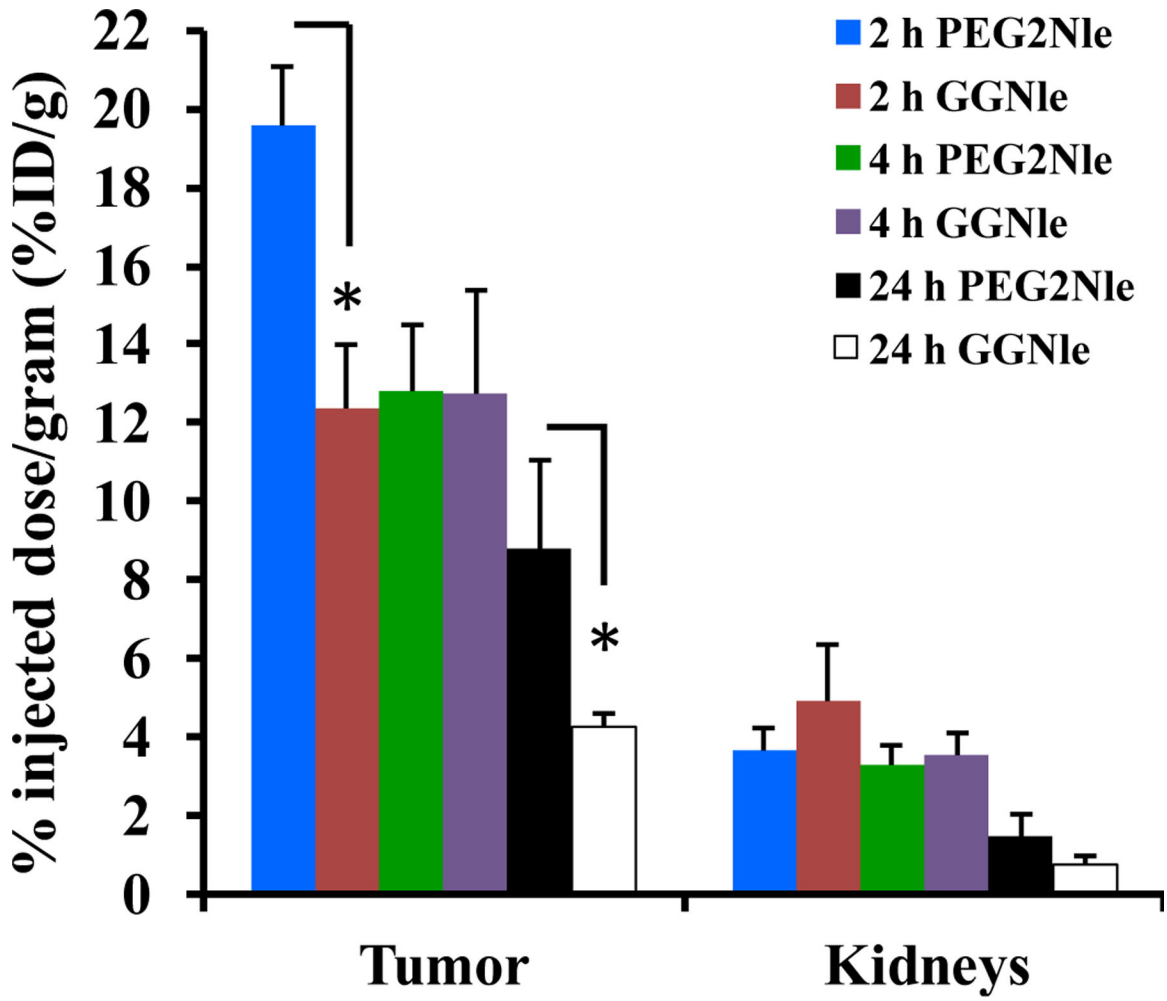

Figure 4.

Comparison of uptake in tumor and kidneys between ^{64}Cu-NOTA-PEG$_2$Nle-CycMSH$_{hex}$ (PEG$_2$Nle) and ^{64}Cu-NOTA-GGNle-CycMSH$_{hex}$ (GGNle) at 2, 4 and 24 h post-injection. The data of ^{64}Cu-NOTA-GGNle-CycMSH$_{hex}$ was cited from our previous publication (ref. 14) for comparison. *p<0.05

Table 1.

Molecular weights (MW) and IC_{50} values of NOTA-PEG_2Nle-CycMSH_{hex} and NOTA-AocNle-CycMSH_{hex} peptides.

Peptide	Calculated MW	Measured MW	IC_{50} (nM)
NOTA-PEG_2Nle-CycMSH_{hex}	1412.6	1412.1	1.24 ± 0.07
NOTA-AocNle-CycMSH_{hex}	1408.8	1408.1	2.75 ± 0.48

Table 2.

Biodistribution of ^{64}Cu-NOTA-PEG$_2$Nle-CycMSH$_{hex}$ on B16/F10 melanoma-bearing C57 mice. The data are presented as percent injected dose per gram (%ID/g) or as percent injected dose (%ID) (means ± SD, n = 4)

Tissues	0.5 h	2 h	4 h	24 h	2 h NDP blockade
Percent injected dose/gram (%ID/g)					
Tumor	16.23 ± 0.42	19.59 ± 1.48	12.83 ± 1.69	8.78 ± 2.29	2.37 ± 0.32 *
Brain	0.24 ± 0.06	0.03 ± 0.01	0.02 ±.0.01	0.04 ± 0.03	0.02 ± 0.02
Blood	3.48 ± 0.95	0.18 ± 0.06	0.20 ± 0.03	0.27 ± 0.10	0.29 ± 0.14
Heart	2.29 ± 0.54	0.19 ± 0.01	0.18 ± 0.06	0.17 ± 0.05	0.21 ± 0.06
Lung	4.04 ± 0.12	0.70 ± 0.04	0.62 ± 0.18	0.69 ± 0.17	0.52 ± 0.14
Liver	2.61 ± 0.55	1.94 ± 0.26	1.95 ± 0.43	1.21 ± 0.23	1.27 ± 0.18
Spleen	1.88 ± 0.67	0.26 ± 0.12	0.41 ± 0.25	0.36 ± 0.17	0.33 ± 0.08
Stomach	2.21 ± 0.56	0.99 ± 0.17	0.92 ± 0.27	0.32 ± 0.15	0.67 ± 0.22
Kidneys	12.14 ± 1.51	3.66 ± 0.52	3.27 ± 0.52	1.47 ± 0.56	4.74 ± 0.48 *
Muscle	1.28 ± 0.39	0.08 ± 0.06	0.03 ± 0.05	0.01 ± 0.01	0.12 ± 0.19
Pancreas	1.10 ± 0.20	0.21 ± 0.13	0.17 ± 0.11	0.01 ± 0.01	0.06 ± 0.05
Bone	2.00 ± 0.42	0.22 ± 0.07	0.19 ± 0.13	0.01 ± 0.01	0.19 ± 0.09
Skin	4.37 ± 1.12	0.40 ± 0.07	0.46 ± 0.22	0.18 ± 0.16	0.43 ± 0.13
Percent injected dose (%ID)					
Intestines	3.26 ± 1.86	1.51 ± 0.23	1.63 ± 0.26	1.24 ± 0.38	1.38 ± 0.44
Urine	44.12 ± 1.85	85.24 ± 3.75	84.17 ± 2.73	88.69 ± 3.18	87.11 ± 2.62
Uptake ratio of tumor to normal tissue					
Tumor/blood	4.66	108.83	64.15	32.52	8.17
Tumor/kidney	1.34	5.35	3.92	5.97	0.50
Tumor/lung	4.02	27.99	20.69	12.72	4.56
Tumor/liver	6.22	10.10	6.58	7.26	1.87
Tumor/muscle	12.68	244.88	427.67	878	19.75
Tumor/skin	3.71	48.98	27.89	48.78	5.51

* $p<0.05$ for determining significance of differences in tumor and kidney uptake between ^{64}Cu-NOTA-PEG$_2$Nle-CycMSH$_{hex}$ with or without peptide blockade at 2 h post-injection.

Table 3.

Biodistribution of ^{64}Cu-NOTA-AocNle-CycMSH$_{hex}$ on B16/F10 melanoma-bearing C57 mice. The data are presented as percent injected dose per gram (%ID/g) or as percent injected dose (%ID) (means ± SD, n = 4)

Tissues	0.5 h	2 h	4 h	24 h	2 h NDP blockade
Percent injected dose/gram (%ID/g)					
Tumor	5.69 ± 0.23	7.71 ± 0.67	5.47 ± 0.52	1.54 ± 0.16	2.03 ± 0.59 *
Brain	0.20 ± 0.08	0.04 ± 0.01	0.02 ±.0.02	0.01 ± 0.01	0.02 ± 0.03
Blood	2.01 ± 0.60	0.27 ± 0.05	0.18 ± 0.07	0.02 ± 0.03	0.38 ± 0.09
Heart	1.49 ± 0.33	0.18 ± 0.05	0.12 ± 0.06	0.22 ± 0.04	0.28 ± 0.11
Lung	3.88 ± 0.71	0.72 ± 0.17	0.36 ± 0.08	0.38 ± 0.06	0.82 ± 0.24
Liver	3.42 ± 0.58	2.19 ± 0.14	0.95 ± 0.21	0.73 ± 0.01	2.20 ± 0.33
Spleen	0.99 ± 0.25	0.17 ± 0.12	0.18 ± 0.09	0.10 ± 0.14	0.34 ± 0.27
Stomach	1.67 ± 0.68	1.69 ± 0.57	0.43 ± 0.09	0.10 ± 0.05	0.74 ± 0.53
Kidneys	30.67 ± 0.94	3.29 ± 0.61	1.08 ± 0.22	0.83 ± 0.11	3.66 ± 0.50
Muscle	0.70 ± 0.18	0.11 ± 0.06	0.03 ± 0.01	0.08 ± 0.02	0.06 ± 0.05
Pancreas	0.75 ± 0.19	0.20 ± 0.18	0.07 ± 0.05	0.02 ± 0.04	0.14 ± 0.13
Bone	1.23 ± 0.34	0.13 ± 0.13	0.08 ± 0.10	0.08 ± 0.14	0.02 ± 0.01
Skin	2.93 ± 0.22	0.39 ± 0.05	0.11 ± 0.06	0.02 ± 0.02	0.21 ± 0.05
Percent injected dose (%ID)					
Intestines	2.12 ± 0.45	3.78 ± 0.51	2.04 ± 0.25	0.74 ± 0.23	2.72 ± 0.45
Urine	56.53 ± 1.07	85.54 ± 3.69	89.41 ± 0.73	96.08 ± 0.39	87.14 ± 1.78
Uptake ratio of tumor to normal tissue					
Tumor/blood	2.82	28.16	30.39	77.0	5.34
Tumor/kidney	0.19	2.34	5.06	1.86	0.55
Tumor/lung	1.47	10.71	15.19	4.05	2.48
Tumor/liver	1.66	3.52	5.76	2.11	0.92
Tumor/muscle	8.13	70.09	182.33	19.25	33.83
Tumor/skin	1.94	19.77	49.73	77.0	9.67

* $p<0.05$ for determining significance of differences in tumor and kidney uptake between ^{64}Cu-NOTA-AocNle-CycMSH$_{hex}$ with or without peptide blockade at 2 h post-injection.